REPORT DOCUMENTATION PAGE

Form Approved
OMB No. 074-0188

1. AGENCY USE ONLY (Leave blank)	2. REPORT DATE	3. REPORT TYPE AND DATES COVERED
	1999	Proceedings

4. TITLE AND SUBTITLE
Spectroscopic Studies of Inhibited Opposed Flow Propane/Air Flames

5. FUNDING NUMBERS
N/A

6. AUTHOR(S)
R.R. Skaggs, R.G. Daniel, A.W. Miziolek, K.L. McNesby, V.I. Babushok, W. Tsang, and M.D. Smooke

7. PERFORMING ORGANIZATION NAME(S) AND ADDRESS(ES)

U.S. Army Research Laboratory, Aberdeen Proving Ground, MD 21005

National Institute of Standards and Technology, Gaithersburg, MD 20899

Department of Mechanical Engineering, Yale University, New Haven, CT 06250

8. PERFORMING ORGANIZATION REPORT NUMBER
N/A

9. SPONSORING / MONITORING AGENCY NAME(S) AND ADDRESS(ES)
SERDP
901 North Stuart St. Suite 303
Arlington, VA 22203

10. SPONSORING / MONITORING AGENCY REPORT NUMBER
N/A

11. SUPPLEMENTARY NOTES

12a. DISTRIBUTION / AVAILABILITY STATEMENT
Approved for public release: distribution is unlimited.

12b. DISTRIBUTION CODE
A

13. ABSTRACT ***(Maximum 200 Words)***

Planar Laser Induced Fluorescence (PLIF) and laser induced fluorescence are used to measure relative OH concentration profiles and maximum flame temperatures in an atmospheric pressure, opposed flow, propane (C_3H_8)/air flame. Flame inhibiting agents CF_3Br, N_2, $Fe(CO)_5$, FM-200, FE-36, DMMP, and PN were added to the flame and relative OH concentration profiles and peak flame temperatures were measured as each flame approached extinction. The OH profiles illustrate that addition of N2, FM-200, and FE-36 to the flame produced smaller changes in OH concentrations relative to CF_3Br implying these agents have chemical inhibition capacities less than CF_3Br. However, the addition of DMMP and $Fe(CO)_5$ to the flame demonstrated chemical inhibition capacities greater than CF_3Br with larger changes in OH concentrations. Similar trends are observed for peak flame temperatures and CF_3Br, PN, DMMP, and $Fe(CO)_5$ have temperature values (1600-1800 K) which are lower than the uninhibited flame peak temperature (2200 K).

14. SUBJECT TERMS
SERDP, SERDP Collection, Planar Laser Induced Fluorescence, PLIF, fire inhibiting agent, Fire protection, FM-200, FE-36, DMMP

15. NUMBER OF PAGES
11

16. PRICE CODE
N/A

17. SECURITY CLASSIFICATION OF REPORT	18. SECURITY CLASSIFICATION OF THIS PAGE	19. SECURITY CLASSIFICATION OF ABSTRACT	20. LIMITATION OF ABSTRACT
unclass	unclass	unclass	UL

NSN 7540-01-280-5500

Standard Form 298 (Rev. 2-89)
Prescribed by ANSI Std. Z39-18
298-102

proceedings of HOTWC-99

SPECTROSCOPIC STUDIES OF INHIBITED OPPOSED FLOW PROPANE/AIR FLAMES

R.R. SKAGGS, R.G. DANIEL, A.W. MIZIOLEK, AND K.L. McNESBY
U.S. Army Research Laboratory
Aberdeen Proving Ground, MD 21005

V.I. BABUSHOK AND W. TSANG
National Institute of Standards and Technology
Gaithersburg, MD 20899

M.D. SMOOKE
Department of Mechanical Engineering
Yale University
New Haven, CT 06250

ABSTRACT

Planar Laser Induced Fluorescence (PLIF) and laser induced fluorescence are used to measure relative OH concentration profiles and maximum flame temperatures in an atmospheric pressure, opposed flow, propane (C_3H_8)/air flame. Flame inhibiting agents CF_3Br, N_2, $Fe(CO)_5$, FM-200, FE-36, DMMP, and PN were added to the flame and relative OH concentration profiles and peak flame temperatures were measured as each flame approached extinction. The OH profiles illustrate that addition of N_2, FM-200, and FE-36 to the flame produced smaller changes in OH concentrations relative to CF_3Br implying these agents have chemical inhibition capacities less than CF_3Br. However, the addition of DMMP and $Fe(CO)_5$ to the flame demonstrated chemical inhibition capabilities greater than CF_3Br with larger changes in OH concentrations. Similar trends are observed for peak flame temperatures and CF_3Br, PN, DMMP, and $Fe(CO)_5$ have temperature values (1600-1800 K) which are lower than the uninhibited flame peak temperature (2200 K). OH profile widths were measured in the uninhibited flame and in each inhibited flame with inhibitor addition at 50 % of determined extinction concentrations. Profiles widths for CF_3Br, PN, DMMP, and $Fe(CO)_5$ were at least 20 % less than the uninhibited flame. Numerical modeling of a stoichiometric, premixed, propane/air flame inhibited by DMMP, $Fe(CO)_5$, CF_3Br, and N_2 indicates DMMP and $Fe(CO)_5$ have greater decreases in burning velocities and OH relative to CF_3Br.

INTRODUCTION

Fire protection on military platforms, including ground fighting vehicles, is being challenged by the impending loss of the ubiquitous fire fighting agent halon 1301 (CF_3Br) due to environmental concerns related to the destruction of the stratospheric ozone layer. Replacement fire extinguishment agents need to be found that will satisfy numerous criteria including: fast fire suppression, minimum production of toxic gases when used, low toxicity, compatibility with storage materials, and environmental acceptability.

The U.S. Army's search for halon replacement agents has largely involved an empirical approach of testing and evaluation of commercially available compounds/systems. An alternative approach is to study the fundamental physical and chemical mechanisms responsible for flame inhibition with the hope that such studies will uncover differences in the flame inhibition mechanisms which will lead to new chemicals for further consideration and testing. To this end, we have initiated planar laser induced fluorescence (PLIF) and laser induced fluorescence (LIF) measurements of the OH radical species as flame extinction was approached in a non-premixed, atmospheric pressure, opposed flow propane/air flame inhibited by halon 1301 [CF_3Br], N_2, $Fe(CO)_5$, FM-200 [C_3F_7H], FE-36 [$C_3F_6H_2$], DMMP [$CH_3P(O)(OCH_3)_2$], and PN [$P_3N_3F_6$]. Presented here are relative OH concentrations, temperatures, and preliminary numerical models from this study of compounds which represent distinctly different chemical families in order to understand the differences between each agent's inhibition mechanism.

BACKGROUND

Chemical inhibition in a flame arises from the lowering of the radical concentrations due to scavenging reactions. In general, efficient inhibition mechanisms contain two types of reactions: a) radical scavenging reactions, and b) reactions regenerating inhibitor species that participate in the inhibition cycle. As an example, for CF_3Br inhibition a free bromine from decomposed CF_3Br forms HBr which chemically reacts with a hydrogen atom and

reduces the flame's hydrogen concentration. The consequence of hydrogen recombination is the overall available radical concentrations (H, O, OH) and the rate of chain-branching reactions are reduced [1,2,3,4] while regeneration of HBr and Br_2 occurs carrying on the inhibition cycle.

The chemicals $Fe(CO)_5$, DMMP, and PN investigated in our laboratory flame system were chosen based on a comprehensive evaluation [5] of fire inhibitors that are more effective than CF_3Br. The inhibition mechanisms for $Fe(CO)_5$, DMMP, and PN are believed to be generally similar to the HBr mechanism. For these postulated mechanisms, each agent decomposes during combustion into inhibition cycle scavenging species, e.g. FeO, FeOH, $Fe(OH)_2$ for $Fe(CO)_5$ addition, [6] and HOPO and $HOPO_2$ for DMMP and PN addition [7,8,9]. In the reaction zone of flames, these scavenging species proceed to behave much like HBr in scavenging hydrogen atoms. FM-200 and FE-36 were studied here due to their popularity as potential candidate halon replacement agents. FM-200 and FE-36 are refrigerants and it is assumed that their primary inhibition capabilities are due to their physical properties of high heat capacities with some chemical reactivity due to CF_3 radical [10].

In order to understand a chemical's inhibition mechanism in terms of physical and/or chemical contributions, both N_2 and CF_3Br are included in this study. That is, N_2 represents the upper boundary for an agent's physical influence on flame inhibition since it has no chemical inhibition capabilities. CF_3Br which has been shown [11] that at least 80 % of its inhibition potential is caused by its chemical properties offers a good intermediate point with which to compare and contrast the other agents studied.

EXPERIMENTAL

OH PLIF imaging measurements were made using the arrangement presented in **Figure 1.**

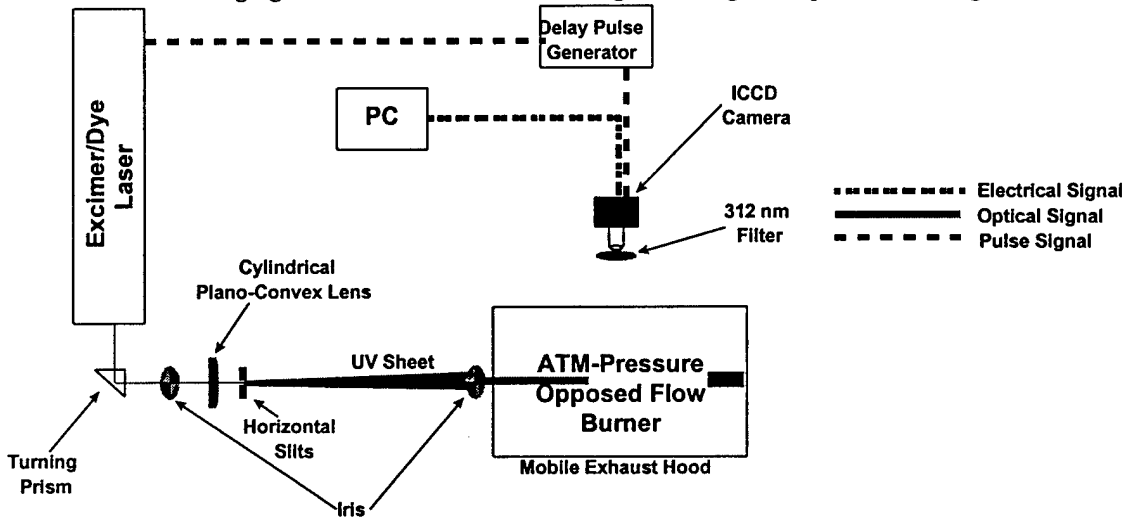

Figure 1: Schematic diagram of the experimental apparatus.

The opposed flow burner apparatus is located inside a stainless steel hood to contain any toxic fumes that are exhausted from the burner. All flames analyzed in this work were studied at atmospheric pressure and consisted of 7.0 L/min synthetic air (79% N_2 + 21% O_2) flowing from the lower duct, and 5.6 L/min of propane flowing from the upper duct. The oxidizer and fuel ducts are separated a distance of 1.2 cm and the duct diameter is 2.54 cm. Based on the flow conditions and duct separation, the luminous flame zone is located on the oxidizer side of the stagnation plane and the global strain rate was calculated to be 72.5 sec^{-1} [12]. Previous studies of non-premixed propane/air flames have experimentally determined global extinction strain rates of 489 s^{-1} [13]. For all studies presented here, the inhibitor agents are added to the oxidizer flow in gaseous form at room temperature with the exception of $Fe(CO)_5$ which was cooled to 11°C and DMMP which was heated to 70°C. Opposed flow burners have been used for some time to study the capabilities of an inhibitor agent because a global parameter, the extinction strain rate [12], can be determined which describes the flame's strength at extinction [14,15,16,17]. The extinction strain rate is useful because a decreased value demonstrates an inhibitor's efficiency. PLIF measurements of radical

concentrations (O, H, OH) are complimentary to the extinction strain rate because the measurements illustrate an inhibitor's influence on the radical concentration profiles in the flame zone which indicates if the flame's radical chemistry is being perturbed by agent addition.

Planar laser induced fluorescence images were measured using a Lambda Physik excimer/dye laser system. This system consists of a Lambda Physik Compex 102 XeCl excimer laser, a Scanmate 2 dye laser (Coumarin 153) and a Second Harmonic Generator (SHG). The fundamental output of the dye laser (560 nm wavelength) was frequency doubled in the SHG unit with a BBO crystal to approximately 281 nm. The UV laser radiation was tuned to the peak of the $R_2(9.5)$ transition at 281.8 nm ((1,0) $A^2\Sigma^+ \leftarrow X^2\Pi$) [18,19,20]. The UV light output of the SHG unit enters an optical train where the beam is turned 90°, apertured by a sub mm iris, projected through a cylindrical plano convex lens to form the UV beam into a vertical sheet. To create a uniform sheet width, the sheet is apertured with 0.5 mm vertical slits as it is projected toward the center of the burner. The UV sheet is apertured just before the burner to produce a vertically uniform intensity that is 1.2 cm in height allowing passage through the entire burner flow field. Laser induced fluorescence from OH passes through a band pass filter centered at 312 nm with a 11 nm bandwidth and is detected with a Princeton Instruments ICCD camera (Model 120) coupled with a Nikon UV lens located at 90° with respect to the UV sheet. The ICCD camera, which has an active area of 384 x 576 pixels, has a field of view with this optical arrangement of approximately 33 cm^2 and each image recorded was acquired with 25 total accumulations on the camera. With this arrangement the entire relative OH concentration profile was obtained.

Laser induced fluorescence excitation spectra were measured in the flame using the Lambda Physik excimer/dye laser system. This arrangement has been utilized before for similar measurements and will only be summarized here [21]. The UV laser radiation was scanned from 281.5 to 282 nm [18,19,20]. Low laser energies were used and the laser was operated in the linear regime. The UV light output of the SHG unit was focused to the center of the burner 30 cm focal length fused silica lens and had a vertical and horizontal beam waist of 0.4 and 0.5 mm, respectively. Fluorescence was collected at 90 degrees to the direction of the excitation laser beam, focused through 0.5 mm iris to define the collection volume, passed through a band pass filter centered at 312 nm with an 11 nm bandwidth, and detected by photomultiplier tube (PMT) (Phillips Model XP2018B).

Before inhibitor addition, the uninhibited flame was profiled using LIF between the fuel and oxidizer ducts to obtain a profile of the uninhibited temperature values. To expedite measurements upon addition of an inhibitor, the burner was translated about ± 1 mm around the OH maximum and excitation spectra were collected. Each excitation spectrum was fit using a non-linear least squares algorithm to obtain the OH rotational temperature for the spectral measurement [22].

RESULTS

The effectiveness of a particular flame inhibitor is typically characterized by its influence on a flame's propagation chemistry. The most common indicators of the overall reaction rates for premixed and diffusion flame systems are the burning velocity and extinction strain rate respectively. For premixed flames, the addition of an inhibitor decreases the burning velocity. For diffusion flames, the addition of an inhibitor can cause chemical reactions to proceed at times near the characteristic flow time which eventually can lead to flame extinction. For premixed and non-premixed systems, measurements of radical concentrations (O, H, OH) serve as useful indicators of the chemistry being affected by inhibitor addition and are complimentary to burning velocity and extinction strain rate measurements. OH is monitored in the flames studied here because it is relatively simple to measure and it is a good indicator of the overall radical pool concentration, even though H, O, and OH have been found to not be fully equilibrated in diffusion flames [23].

Figure 2 presents two representative, two-dimensional images of OH fluorescence for an uninhibited propane/air flame and for a propane/air flame to which CF_3Br was added (1.5 % by volume). Both images, which are uncorrected for laser energy fluctuations and local quenching rates, illustrate the presence of two luminous zones as the UV sheet passes through the flame. The lower, thicker zone is the fluorescence from the OH transition while the upper, thinner zone is the broadband fluorescence due to derivative fuel species such as polycyclic aromatic hydrocarbons. To construct a spatially resolved OH LIF profile from a OH PLIF image, as shown on the

right hand side of **Figure 2**, the pixel intensity corresponding to a given height between the fuel and oxidizer ducts (spatial resolution approximately 0.149 mm/pixel) was summed and averaged over a 1 mm horizontal width. The two-dimensional images and LIF profiles illustrate that addition of CF_3Br to the propane flame causes a decrease in the OH fluorescence signal while the broadband fluorescence appears to increase just slightly. Similar results have been observed previously for CF_3Br addition to hydrocarbon diffusion flames [24,25].

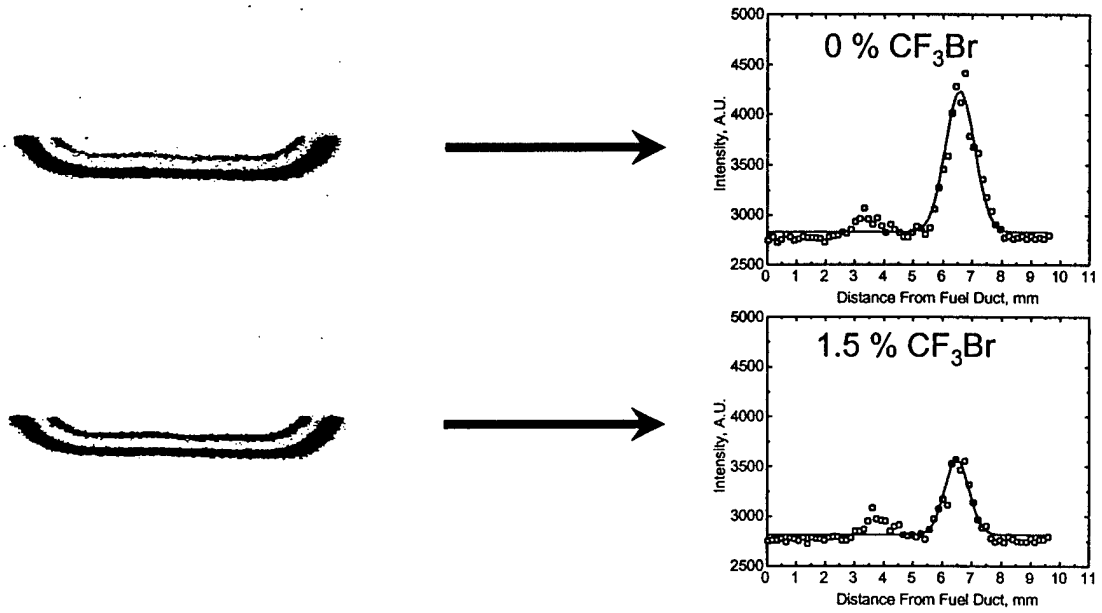

Figure 2: Representative PLIF images and the corresponding OH intensity profiles from an opposed flow propane/air flame seeded with 0 % (by volume) CF_3Br and 1.5 % (by volume) CF_3Br. Note: The orientation of the PLIF images with respect to the burner system places the fuel and air ducts at the top and bottom of each image respectively.

Obviously the addition of an inhibitor to a flame gives rise to modifications in the flame structure. Specifically, addition of an inhibitor can change the position and width of the flame's reaction zone. Previous studies have shown [26,27,28,29,30] that a decrease in the flame's reaction zone width indicates increased localized strain, which can cause local quenching or flame extinction [31]. For the analysis of reaction zone modifications and relative OH concentrations, each OH intensity profile is fit to a gaussian function. A gaussian function determines the area under the profile curve which provides a general indicator of the entire OH population for a given flame condition. The width of the flame's reaction zone may be characterized by the width of a radical profile [30]. The width of the flame's reaction zone is defined here as the distance of one half of the maximum intensity of the gaussian OH profile which is similar to previous studies [28] that have estimated the width of a laminar flame reaction zone using one half of the maximum value of a temperature profile.

Figure 3 contains the results of the analyzed OH profile areas versus each inhibitor agent's concentration as the flames were stepped towards extinction. The reported OH profile areas are averaged over three or more separate inhibitor extinction experiments, where the data for each experiment are normalized to the OH profile area measured in the uninhibited flame acquired prior to each inhibitor extinction experiment to account for changes in burner and camera conditions. The data indicate that there are both physical and chemical modes of inhibition being observed for the agents studied. That is, N_2 which is chemically inert has the least impact on OH with respect to the other agents studied. For the concentration range plotted in **Figure 3** the flame was not even extinguished by N_2. Similar results are observed for the two fluorinated propanes (FM-200 and FE-36) which show initially small declines in OH, but more rapid decreases just before extinction. For the other agents studied (PN, CF_3Br, DMMP, and $Fe(CO)_5$), the addition of these inhibitors show precipitous decreases in the measured OH

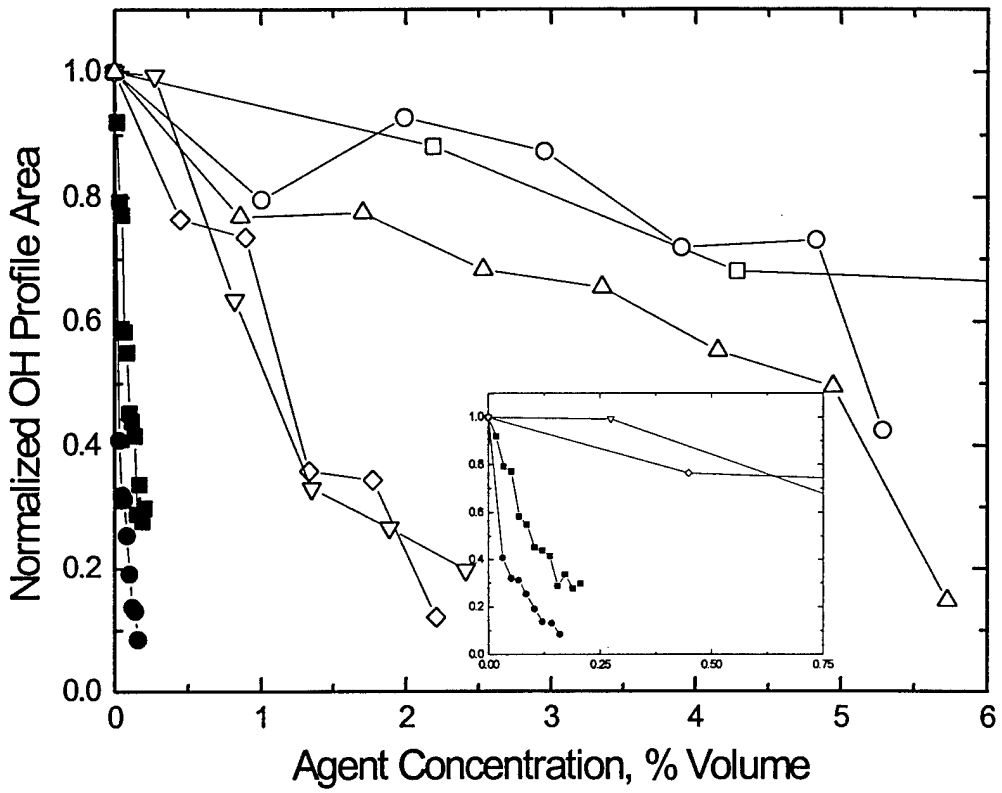

Figure 3: Normalized OH LIF profile areas versus inhibitor agent delivery concentrations. The ( )) are the N_2 data, the ( ) are the FM-200 data , the (+) are the FE-36 data, the (,) are the PN data, the (( ) are the CF_3Br data, the (■) are the DMMP data, and the (●) are the $Fe(CO)_5$ data. Inserted in the figure is a second plot of the PN, CF_3Br, DMMP, and $Fe(CO)_5$, data for agent concentration up to 0.75 % volume.

values up to the extinction concentrations where the data seems to decrease more gradually, as highlighted for DMMP and $Fe(CO)_5$ with the inserted graph in **Figure 3**. **Table I** lists the observed inhibitor concentrations in the air stream at extinction for each agent studied here and their estimated uncertainties.

Table I: Inhibitor concentrations (% volume) and uncertainty (± % volume) at flame extinction

Inhibitor Agent	**N_2**	**CF_3Br**	**FE-36**	**FM-200**	**PN**	**DMMP**	**$Fe(CO)_5$**
Extinction Concentration	23.1	2.3	6.1	5.3	2.7	0.3	0.2
Estimated Uncertainty	8.20	0.93	1.29	1.08	1.00	0.04	0.03

For comparison purposes, the extinction concentration for CF_3Br is similar to cup burner values (2.90) [32], but slightly less than values obtained in a co-flowing propane/air flame and a co-flowing propane/air cup burner (4.1 and 4.3) [25,33]. The fluorinated propanes have extinction concentrations that are approximately 50 % greater than CF_3Br, which is consistent with cup burner values of 6.3 and 6.6 for FM-200 and FE-36 respectively [32]. For the phosphorus compounds, PN has an extinction concentration similar to CF_3Br while DMMP's value is significantly less than CF_3Br (7 - 8 times less). Previous studies by MacDonald et al. [34,35] have shown DMMP to be 2 - 4 times more effective than CF_3Br. However, Fisher et al. [13] have reported for an opposed flow propane/air flame with DMMP added to the air stream, a 25 % decrease in the normalized extinction strain rate corresponds to a DMMP concentration ≈ 1200 ppm. Linear extrapolation of the cited Fisher et.al. data [13] to the strain rate used for the opposed flow, propane/air flame studied here finds a DMMP concentration of 4080 to 6500 ppm or 0.4-0.65 %

volume. The DMMP concentration obtained from the extrapolated strain rate data supports the DMMP extinction concentration determined here. For PN, cup burner experiments have found an extinction concentration of 1.08 [36]. The results reported here for PN and DMMP are concerning for several reasons. First the obtained value for PN is larger while DMMP is smaller than other cited experiments. Second, it was assumed prior to the experiments described here, that if a given compound contained a phosphorus atom, that regardless of its chemical structure similar extinction concentrations would be observed. A possible explanation for the contrasting behavior between the two phosphorus agents is the resonant structure of PN could be very stable and thus less efficient at delivering phosphorus to the flame [37].

One of the conveniences of monitoring relative OH concentration profiles using a PLIF technique is that any physical changes that occur in the OH profile are observed instantaneously as the inhibitor agents are added. This quality is convenient because the addition of an inhibitor to the flame gives rise to modifications in the flame structure such as shifting the location of the OH maximum and/or effecting the OH profile width. **Table II** lists the measured flame widths determined from the relative OH concentration profiles for each flame situation studied. For the inhibited flames, the widths are measured at 50 % of each agent's determined extinction concentration. The uncertainty in the reported widths due to measurement variance is 11 %.

Table II: Measured OH profile widths (FWHM, mm) for the uninhibited flame and inhibited flames at 50 % of the inhibitor extinction concentrations.

	OH Profile Width, mm
Uninhibited	1.30
N_2	1.24
FE-36	1.31
FM-200	1.26
CF_3Br	0.96
PN	0.96
DMMP	1.04
$Fe(CO)_5$	0.83

The **Table II** width values indicate that the agents, N_2, FE-36, FM-200 do not posses width changes significantly different than the uninhibited flame. On the contrary CF_3Br, PN, DMMP, and $Fe(CO)_5$ exhibit width changes that are equal to or greater than a 20 % decrease from the uninhibited width value. The OH width trends suggest that inhibitor agents with more physical inhibition capabilities exhibit less effect on the flame structure than inhibitors with enhanced chemical inhibiting capabilities.

From the relative OH concentration observations, similar trends might be expected for the peak flame temperatures. **Figure 4** presents a plot of peak LIF measured flame temperatures versus agent delivery concentrations for each inhibited flame. The peak flame temperature for the uninhibited flame is between 2125 and 2200 K. The obtained temperature values for N_2 and FM-200 indicate that these inhibited flames do not have temperatures statistically different from those measured in the uninhibited flame with an estimated uncertainty of $\pm$ 300 K. For CF_3Br and PN, temperature differences with respect to the uninhibited flame are not observed until near extinction concentrations are achieved. Previous studies of an atmospheric pressure, axi-symmetric propane/air flame inhibited by addition of CF_3Br to the oxidizer flow, found only small temperature differences in comparison with the uninhibited flame [25,38]. On the contrary, Masri et al. [24] report for a non-premixed atmospheric pressure CH_4/air flame that higher temperatures exist in the reaction zone of a CF_3Br inhibited flame than in the reaction zone of an uninhibited flame near extinction. With mixed results from previous investigations and the large degree of uncertainty in our measurements, the only creditable temperature values are those close to extinction. For $Fe(CO)_5$ and DMMP temperature decreases with respect to the uninhibited flame are not observed until proximal extinction concentrations are observed as well. On a concentration basis, $Fe(CO)_5$ and DMMP have decreased flame temperatures, $T \approx 1700$ K, at agent concentrations lower than the other agents studied. For $Fe(CO)_5$, small decreases in flame temperatures have been observed by Brabson et al. [39] in studies of low-pressure premixed flames inhibited by $Fe(CO)_5$.

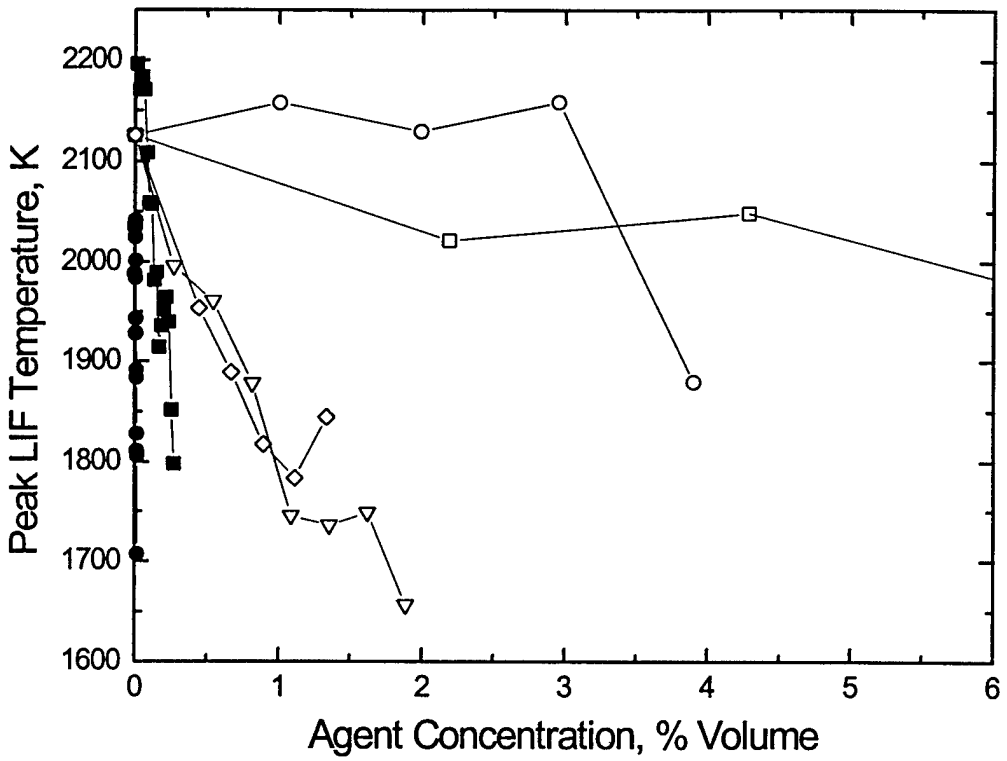

Figure 4: Peak LIF measured temperatures (K) versus inhibitor agent delivery concentrations. The ( )) are the N_2 data, the ( ) are the FM-200 data , the (,) are the PN data, the (( ) are the CF_3Br data, the (■) is the DMMP data, and the (●) are the $Fe(CO)_5$ data.

NUMERICAL MODELING

Numerical modeling of a stoichiometric, premixed, propane/air flame inhibited by DMMP, $Fe(CO)_5$, CF_3Br, and N_2 flame was carried out using the Chemkin suit of programs [40]. For the simulations, a kinetic model for propane combustion developed by Marinov et.al. [41,42,43] was slightly modified and combined with a C1-C2 hydrocarbon kinetic model [11] that has been employed in earlier inhibition studies. For routine calculations, a simplified model was used to decrease computational time. The kinetic mechanism for phosphorus containing species is based on the model suggested for the analysis of the influence of PH_3 products on the recombination of hydroxyl and hydrogen atoms in a hydrogen flame [44], and kinetic models [45,46,47] developed to simulate destruction of DMMP and TMP in low pressure hydrogen flame. Additional reactions were added to the phosphorus mechanism to complete the reaction pathways for the consumption of some of the P containing species. For the modeling of $Fe(CO)_5$ and CF_3Br inhibition, previously developed mechanisms for these two species [6,1] were added to the hydrocarbon model.

Computations of the propane flame inhibited by DMMP demonstrate that the consumption of DMMP leads via a sequence of reactions to the formation of CH_3PO_2 species. Reactions of CH_3PO_2 with H and OH create HOPO and $HOPO_2$ species. At this stage, reactions of HOPO, $HOPO_2$, and PO_2 with chain carriers form the following two inhibition cycles:

1) $H + PO_2 + M = HOPO + M$
$OH + HOPO = H_2O + PO_2$
$H + HOPO = H_2 + PO_2$
$O + HOPO = PO_2 + OH$

2) $OH + PO_2 + M = HOPO_2 + M$

$H + HOPO_2 = H_2O + PO_2$

These inhibition cycles represent the catalytic scavenging cycles that accelerate radical recombination in combustion products containing phosphorus compounds [9]. It is well known that the addition of an inhibitor decreases the burning velocity for premixed flames. Numerical results for burning velocity decreases of 20-30 % using the original rate constants given by Twarowski [9], indicate that DMMP decreases the flame's burning velocity by a factor of 1.5 - 2 relative to CF_3Br in a methane/air flame. Sensitivity analysis reveals that the burning velocity is receptive to changes in the rate constants for the reactions of PO2 radical: $H + PO_2 + M = HOPO + M$ and $OH + PO_2 + M = HOPO_2 + M$. Reasonable adjustment of rate constants can lead to agreement with experimental data.

It should be noted that phosphorus compounds have a wide range of thermal stability. Activation energies of decomposition reactions are in the range 15 - 90 kcal/mol. The influence of the decomposition rate was studied using global kinetics for the decomposition to PO_2 to HOPO species by varying of overall activation energy for the decomposition reaction. Calculations show that for the compounds with global activation energies less than 50 kcal/mol, the burning velocity is not effected by the stability of the phosphorus compounds.

Suppression calculations were carried out with increasing additive loadings until suppression concentration levels were achieved (burning velocity ≤ 5 cm/sec [2]). It should be noted that the calculations were conducted for a gas phase model without taking into account possible condensation processes. Calculation results, **Figure 5**, show that DMMP appears to have less effect in reducing the burning velocity in comparison with $Fe(CO)_5$, but relative to CF_3Br both are more effective. For increases in the concentration of $Fe(CO)_5$ and DMMP, both agents exhibit increasing saturation effects. Typically, two types of saturation are discussed in the literature: 1) saturation of chemical influence [11], and 2) saturation due to condensation processes [6].

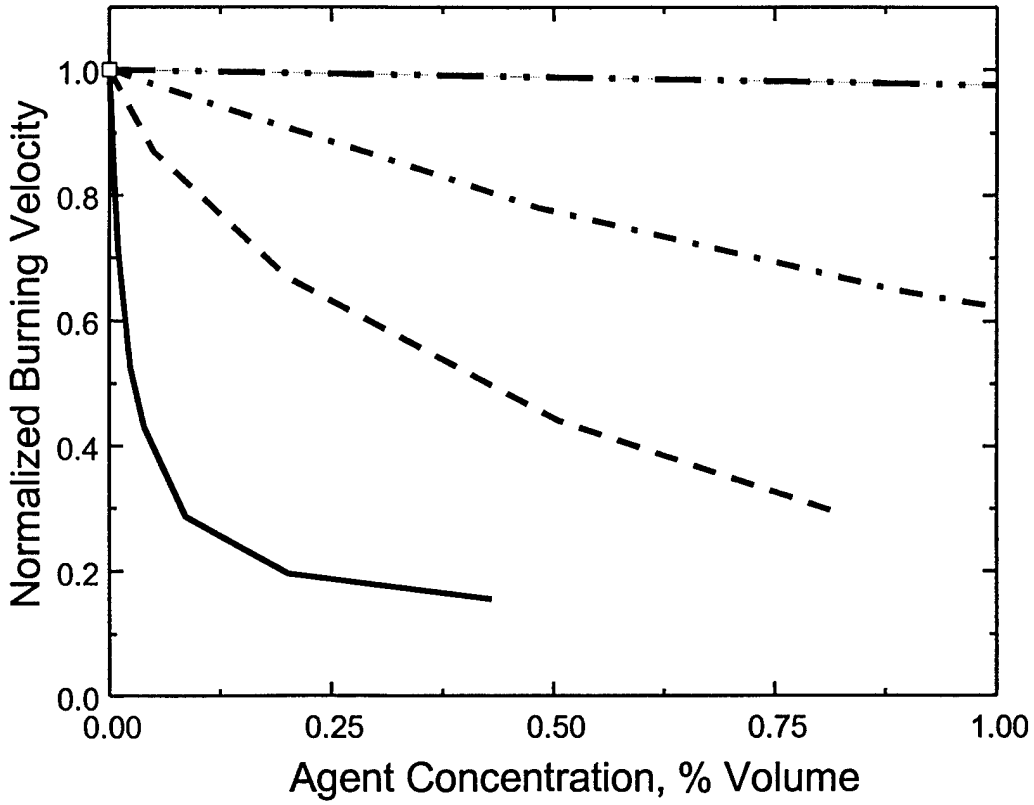

Figure 5: Calculated burning velocities versus delivered inhibitor agent concentrations for a numerical, stoichiometric, premixed, propane/air flame. The dashed line is the DMMP data, the solid line is the $Fe(CO)_5$ data, the dashed dot dashed line is the CF_3Br data, and the near horizontal dashed dot dot dashed line represents the N_2 data trend.

Both processes result in a decrease in inhibitor efficiency with increased inhibitor concentration. For example, to decrease the burning velocity to 10cm/s requires a DMMP loading of approximately 0.9 %, but an additional 1.2 % of DMMP is needed to decrease the burning velocity to the extinction level of 5 cm/s. Such a strong saturation effect leads to a substantial increase in extinction concentrations and a decrease in inhibitor efficiency relative to CF_3Br. The calculated extinction concentrations, in units of % volume, for the numerical propane/air flame were: DMMP = 2.1; $CF_3Br \approx 3.5$; $Fe(CO)_5 = 0.4\text{-}0.5$ and $N_2 \approx 40$. The modeling results support that DMMP and $Fe(CO)_5$ exhibit superior inhibition capabilities relative to CF3Br.

Finally comparison of the normalized OH concentrations dependency on inhibitor concentrations demonstrates a correlation between experimental and calculated OH concentrations, **Figure 6. Figure 6** illustrates that two different propane flames inhibited by the same agents have normalized OH concentrations that track more or less with one another. At the experimental OH extinction level, i.e. 0.3 to 0.1, both data sets (experimental/computational) have similar normalized OH reductions.

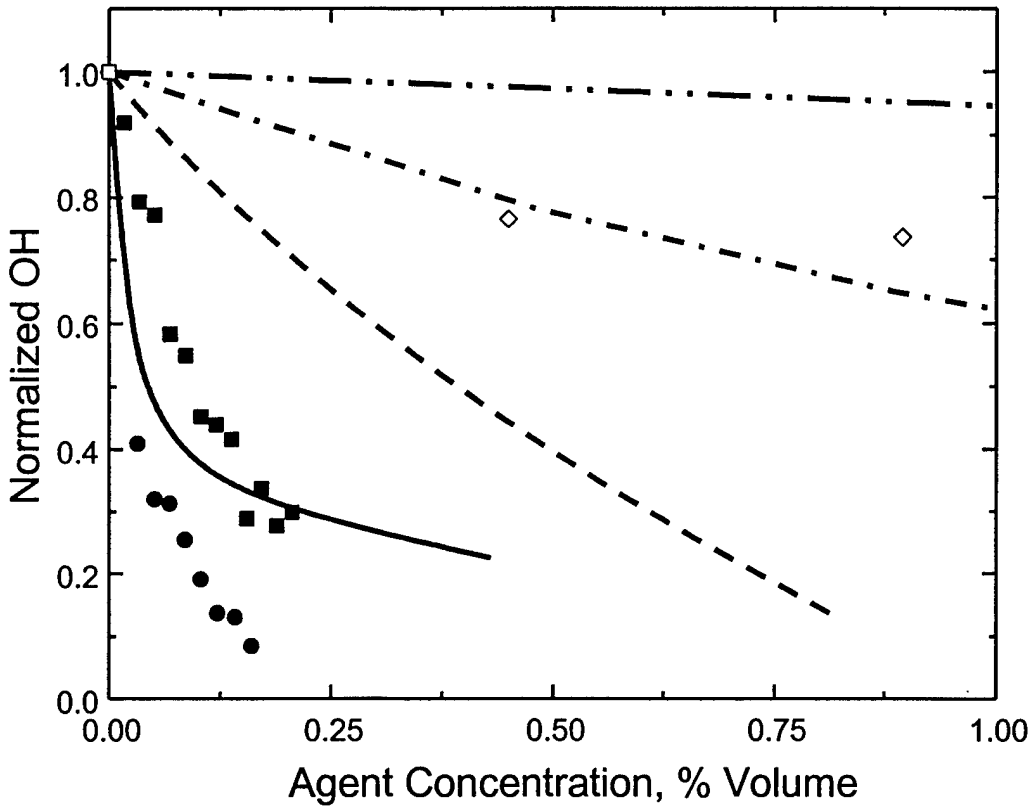

Figure 6: Normalized OH concentrations versus delivered inhibitor agent concentrations. The (●) are the experimental $Fe(CO)_5$ data and the solid line is the numerical $Fe(CO)_5$ data; the (■) are the experimental DMMP data and the dashed line is the numerical DMMP data; the (◇) are the experimental CF_3Br data and the dashed dot dashed line is the numerical CF_3Br data. The near horizontal dashed dot dot dashed line represents the N_2 data trend.

CONCLUSIONS

The experimental results presented here show for the first time changes in OH profiles as extinction is approached in a series of inhibited, atmospheric pressure, non-premixed, propane/air flames. The OH profiles from these flames illustrate that N_2, FE-36, and FM-200, with smaller changes in OH areas relative to CF_3Br, exhibit chemical inhibition capacities less than CF_3Br. On the contrary, DMMP and $Fe(CO)_5$ demonstrate chemical inhibition capabilities greater than CF_3Br with their larger changes in OH. Peak flame temperature measurements demonstrate that inhibitor additions cause temperature values to decrease with similar trends as the relative OH concentrations. For the inhibitors studied, agent concentrations at extinction support these observations with a CF_3Br concentration of 2.3 % (by volume) compared to N_2 with a concentration of 23.1 % and DMMP and $Fe(CO)_5$ each having concentrations less than 1 %. Analysis of the OH profile widths for flames inhibited by $Fe(CO)_5$,

DMMP, CF_3Br, and PN show the OH profiles widths are less than those experienced in the uninhibited flame. Contrariwise, flames inhibited by N_2, FM-200, and FE-36 do not demonstrate profile widths much different than those observed for the uninhibited flame. Numerical calculations for a stoichiometric, premixed, propane/air flame demonstrate that DMMP and $Fe(CO)_5$ exhibit superior inhibition characteristics relative to CF_3Br.

ACKNOWLEDGMENTS

The authors would like to thank Anthony Hamins (NIST) for burner fabrication. This work was supported by the Next Generation Fire Suppression Technology Program under the auspices of the U.S. Army TACOM (Steve McCormick). Finally R. Skaggs would like to acknowledge financial support from the Army Research Laboratory through an American Society for Engineering Education Postdoctoral Fellowship.

REFERENCES

1. Dixon-Lewis, G., Simpson, R.J., *Sixteenth Symposium (International) on Combustion,* The Combustion Institute, Pittsburgh, 1976, p.1111.
2. Westbrook, C.K. *Combust. Sci. Technol.* 23: 191 (1980).
3. Westbrook, C.K. *Nineteenth Symposium (International) on Combustion,* The Combustion Institute, Pittsburgh, 1982, p.127.
4. Westbrook, C.K. *Combust. Sci. Technol.* 34: 201 (1983).
5. Babushok, V., and Tsang, W. *Chemical and Physical Processes in Combustion: Proceedings of Fall Technical Meeting of the Eastern States Section of the Combustion Institute*, 1997, p.79.
6. Rumminger, M.D., Reinelt, D., Babushok, V.I., and Linteris, G.T., *Combust. Flame* 116: 207 (1999).
7. Hastie, J.W. and McBee, C.L. National Bureau of Standards, Final Report No. NBSIR 75-741, (1975).
8. Twarowski, A., *Combust. Flame* 94: 91 (1993).
9. Twarowski, A., *Combust. Flame* 102: 41 (1995).
10. Williams, B.A., Fleming, J.W., and Sheinson, R.S., *Halon Options Technical Working Conference*, Albuquerque, 1997, p.31.
11. Noto, T., Babushok, V., Burgess, D.R., Hamins, A., Tsang, W., Miziolek, A., *Twenty-Sixth Symposium (International) on Combustion*, Pittsburgh 1996, p.1377.
12. Seshadri, K. and Williams, F., *Int. J. Heat and Mass Tarnsfer* 21:251 (1978).
13. Fisher, E.M., Gouldin, F.C., Jayaweera, T.M., and MacDonald, M.A, "Flame Inhibition by Phosphorus-Containing Compounds" Final Technical Report distributed by Defense Advanced Research Projects Agency, Arlington, VA, (1998).
14 Potter, A.E., Heimel, S., and Butler, J.N., *Eighth Symposium (International) on Combustion*, The Combustion Institute, Pittsburgh, 1962, p.1027.
15. Carrier, G.F., Fendell, F.E., and Marble, F.E., SIAM *J. Appl Math.* 28: 463-500 (1975)
16. Linan, A. *Acta Astronaut* 1: 1007 (1974).
17. Williams, F.A. *Fire Saf. J.* 3:163 (1981)
18. Chidsey, I.L., and Crosley, D.R., *J. Quant. Spectrosc. Radiat. Transf*, 23: 187 (1980)
19. Dieke, G.H., and Croswhite, H.M., *J. Quant. Spectrosc. Radiat. Transf.* 2: 97 (1962).
20. Kotlar, A., Private Communication (1998).
21. Skaggs, R.R., McNesby, K.L., Daniel, R.G., Homan, B., and Miziolek, A.W., submitted to *Combust. Sci. and Technol.*, (1999).
22. Kotlar, A., Ph.D. Thesis (1978).
23. Smyth, K.C., Tjossem, P.J.H., Hamins, A., and Miller, J.H., *Combust. Flame* 79: 366 (1990).
24. Masri, A.R., Dally, B.B., Barlow, R.S., and Carter, C.D., *Combust. Sci. Technol.* 113-114: 17 (1996).
25. Smyth, K.C., and Everest, D., *Twenty-Sixth Symposium (International) on Combustion*, The Combustion Institute, Pittsburgh, 1996, p.1385.
26. Peters, N. *Combust. Sci. Technol.* 30: 1 (1983).
27. Liew, S.K., Bray, K.N.C., and Moss, J.B., *Combust. Flame* 56: 199 (1984).
28. Haworth, D.C., Drake, M.C., and Blint, R.J., *Combust. Sci. Technol.* 60: 287 (1988).
29. Roberts, Wm. L., Driscoll, J.F., Drake, M.C., and Ratcliffe, J.W., *Twenty-Fourth Symposium (International) on Combustion*, The Combustion Institute, Pittsburgh, 1992, p.169.

30. Miller, J.H., *Chemical and Physical Processes in Combustion: Proceedings of Fall Technical Meeting of the Eastern States Section of the Combustion Institute*, 1996, p.1.
31. Bilger, R.W. *Twenty-Second Symposium (International) on Combustion*, The Combustion Institute, Pittsburgh, 1988, p.1377.
32. *Cup-Burner Flame Extinguishment Concentrations*, NMERI Report http://www.nmeri.unm-cget, (1998).
33. Grosshandler, W.L., Gann, R.G., and Pitts, W.M., "Evaluation of Alternative In Flight Fire Suppresants for Full Scale testing in Simulated Aircraft Engine Nacelles and Dry Bays," NIST SP 861, (1994).
34. MacDonald, M.A., Jayaweera, T.M., Fisher, E.M., Gouldin, F.C. *Combust. Flame* 116: 166 (1999).
35. MacDonald, M.A., Jayaweera, T.M., Fisher, E.M., Gouldin, F.C. *Twenty-Seventh Symposium (International) on Combustion*, 1998, in press.
36. Kaizerman, J.A., and Tapscott, R.E. *Advanced Streaming Agent Development, Volume III: Phosphorus Compounds*, New Mexico Engineering Research Institute, Report No. NMERI 96/5/32540, (1996).
37. Gann, R., Private Communication (1999).
38. Niioka, T, Mitani, T., and Takahashi, M., *Combust. Flame* 50: 89-97 (1983).
39. Brabson, G.D., Walters, E.A., Gennuso, A.R., Owen, J.P., and Tapscott, R.E. submitted *J. Phys. Chem.*, (1998).
40. Kee, R.J., Rupley, F.M., and Miller, J.A., Chemkin-II: A Fortran Chemical Kinetics Package for Analysis of Gas Phase Chemical Kinetics. Sandia National Laboratories Report No. SAND-8009B, UC-706, (1989).
41. Marinov, N.M., Pitz, W.J., Westbrook, C.K., Castaldi, M.J., Senkan, S.M. *Combust.Sci.Technol.*, 116-117: 211 (1996).
42. Marinov, N.M., Castaldi, M.J., Melius, C.F., Tsang, W. *Combust.Sci.Technol.*, 128: 295 (1997).
43. Marinov, N.M., Pitz, W.J., Westbrook, C.K., Vincitore, A.M., Castaldi, M.J., Senkan, S.M. *Combust.Flame*, 114: 192 (1998).
44 Ewing, C.T., Hughes, J.T., Carhart, H.W. *Fire and Materials* 8(3), 148 (1984).
45. Werner, J.H., Cool, T.A., *Combust. Flame* 117: 78 (1998).
46. Korobeinichev, O.P., Il'in, S.B., Mokrushin, V.V., Shmakov, A.G. *Combust.Sci.Technol.* 116-117:51 (1996)
47. Mokrushin, V.V., Bol'shova, T.A., Korobeinichev, O.P. "A Kinetic Model for the Destruction of TMP in a Hydrogen/Oxygen Flame," unpublished data.